A New Graphical Device and Related Tests for the Shape of Non-parametric Regression Function

Subhra Sankar Dhar[1], Prashant Jha[2], Mohammad Arshad Rahman[3], and Joydeep Dutta[4]

[1]Department of Mathematics and Statistics, IIT Kanpur, India
[2]Department of Mathematics and Statistics, IIT Kanpur, India
[3]Department of Economics, IIT Kanpur, India
[4]Department of Economics, IIT Kanpur, India

October 8, 2019

Abstract

We consider a non-parametric regression model $y = m(x) + \epsilon$ and propose a novel graphical device to check whether the r-th ($r \geqslant 1$) derivative of the regression function $m(x)$ is positive or otherwise. Since the shape of the regression function can be completely characterized by its derivatives, the graphical device can correctly identify the shape of the regression function. The proposed device includes the check for monotonicity and convexity of the function as special cases. We also present an example to elucidate the practical utility of the graphical device. In addition, we employ the graphical device to formulate a class of test statistics and derive its asymptotic distribution. The tests are exhibited in various simulated and real data examples.

Keywords: Convex Regression; Derivatives of Regression Function; Hypothesis Testing; Isotonic Regression

2010 *Mathematics Subject Classification.* Primary: 62G08, 62G10; Secondary: 62M99

1 Introduction

The estimation of shape restricted regression function (particularly, isotonic regression function) is an old and well explored problem in the literature on non-parametric statistics. Inference on this topic can be traced to Hildreth (1954) and Brunk (1955). Later in Barlow, Bartholomew, Bremmer, and Brunk (1972) and Barlow and Brunk (1972), the problem is discussed in the context of regression. They consider the optimization problem to find the least squares estimate and its dual problem, which in several cases simplifies the optimization problem (see Dhar (2016) for details). Quadratic loss under normality is investigated in C.-I. C. Lee (1981). Algorithms to find isotonic data points and regression function are studied in several articles including Dykstra (1981), Dykstra and Robertson (1982), C.-I. C. Lee (1983), Best and Chakravarti (1990) and Dette, Neumeyer, and Pilz (2006). For convex regression, Lim and Glynn (2012) investigates the consistency property of the least squares estimator.

Beyond the theoretical and methodological interests, assuming a specific shape (e.g., monotonicity or convexity) of the non-parametric regression function is common in a wide class of applications across disciplines. For instance, monotone relationship has been extensively used to model growth curves in Biology. In environmental sciences, an isotonic function is often used to model the number of days until freezing of a lake (see Bhattacharya and Klotz (1966)). Among other shape restrictions, the 'production function' used in economics is a concave function (see Varian (1992)). More generally, interest often lies in feature of derivatives of the regression function since *the shape of a function can be characterized by a specific order of the derivative of the function.* Additionally, the shape of data is often not apparent from the scatter plots (or other visual depiction) of the data. Motivated by these challenges in theory and applications, this paper proposes a graphical device to correctly identify the shape of the regression function. The graphical device is further employed to derive a class of test statistics and find its asymptotic distribution. The graphical device and tests are exhibited in several simulated and real data examples.

This paper contributes to at least two growing statistical literatures – graphical device

to display data characteristics, and tests to examine shape of regression function. With respect to the former, there have been a few attempts to propose visualization tool to display the data characteristics. For example, Friedman and Rafsky (1981) study graphical device for multivariate two sample problem using the idea of minimal spanning tree. Easton and McCulloch (1990) propose multivariate quantile-quantile plots using the concept of matching. Bivariate quantile-quantile plots using geometric quantile are presented in Marden (1998) and Marden (2004), and multivariate quantile-quantile plots using geometric quantiles is proposed in Dhar, Chakraborty, and Chaudhuri (2014). However, the graphical devices in the above mentioned articles cannot investigate regression function and its derivatives, which is the primary contribution of the current article.

The literature on testing shape of regression function is quite sparse. Ghosal, Sen, and Van Der Vaart (2000) proposed test statistics for examining monotonicity of non-parametric regression function. However, since their focus is only on monotonicity property (i.e., $r = 1$), they did not consider derivatives of the regression function. Besides, no visualization tool is presented to for validating their assertion. In our approach, the test statistics and the theoretical results associated with the graphical device involve a certain process or a specific functional of the process. Hence, our theoretical results boils down to establishing the asymptotic properties of the given process. As we deal with the r-th derivative of the regression function, the process involves the $(r-1)$-th order derivative of the kernel based estimator of the unknown regression function, which makes the problem theoretically more challenging. We overcome these challenges using a few advanced results of kernel based estimator of the regression function.

This paper contributes to the two literatures by introducing a graphical device to identify the shape of the regression function, and subsequently utilize the graphical device to formulate a class of test statistics and derive its asymptotic distribution. For a function, sufficiently smooth, its shape can be completely characterized by the sign of a certain order derivative. This is utilized to propose a graphical device based on the concept of concordance-discordance and correctly identify the shape of the regression function. In particular, the aim is to check whether r-th ($r \geq 1$) derivative of the unknown regression

function is positive or not. Note that monotonicity (i.e., $r = 1$) and convexity (i.e., $r = 2$) of the function are simply special cases of the more general method proposed here. In addition, the graphical device is utilized to construct a class of test statistics which can be used to test the shape of the regression function and also derive the asymptotic distribution of the proposed test. The tests are demonstrated in multiple simulations and implemented to study some popular real data examples.

The rest of this article is organized as follows. We propose the graphical device in Section 2, and Section 2.1 contains a few diagrams to illustrate about how our proposed graphical device works for various examples. In Section 3, the corresponding testing of hypothesis is considered, and the test statistics are formulated. Section 3.1 investigates the asymptotic distributions of the formulated test statistics. The performance of the proposed tests are studied for a few simulated and real data examples in Section 4, and Section 5 presents concluding remarks. The Appendix contains all the technical details.

2 Proposed Graphical Device

We consider a nonparametric regression model $y_i = m(x_i) + \epsilon_i$, for all $i = 1 \ldots n$, where y_i is the response, x_i is the fixed scalar covariate, and ϵ_i is the error corresponding to the i-th observation. The function $m(\cdot)$ is unknown and has nonparametric form. To avoid the problem of identification, it is assumed that $E(\epsilon) = 0$ and to maintain the noise to a reasonable level, we also assume that $E(\epsilon^2) < \infty$.

We are interested in testing the hypothesis $H_0 : m^{(r)}(\cdot) > 0$, where $r = 1, 2, \ldots$, and this assertion implies the existence of r-th order derivative of m (which is denoted by $m^{(r)}$). In other words, it follows from the result in calculus that the null hypothesis can be rephrased as $H_0 :$ $m^{(r-1)}(\cdot)$ is an increasing function. Strictly speaking, it is equivalent to the statement that $\left(m^{(r-1)}(x) - m^{(r-1)}(y)\right) \times (x - y)$ is positive for all possible values of x and y, and this fact is used to construct the graphical device and formulate the test statistics. Intuitively speaking, under H_0, $\sum_{1 \leqslant k \neq i \leqslant n} sign\left\{\left(m^{(r-1)}(x_i) - m^{(r-1)}(x_k)\right)(x_i - x_k)\right\}$ is expected to be greater than zero, where $sign(x) = \dfrac{x}{|x|}$ if $x \neq 0$, and $= 0$, otherwise.

However, $m^{(r-1)}(\cdot)$ involved in the above expression is unknown in practice, and hence, one cannot use this expression directly in data analysis. In order to take care of this issue, one can plug in a consistent estimator of $m^{(r-1)}$ in the expression to implement the method. The literature offers a few well-known consistent estimators of the regression function and its derivatives: Here we consider the Gasser-Muller estimator, for its tractable expression. The Gasser-Muller estimator is defined as

$$\hat{m}_n(t) = \frac{1}{h_n} \sum_{j=1}^{n} y_j \int_{s_{j-1}}^{s_j} K\left(\frac{t-u}{h_n}\right) du, \tag{1}$$

where $\{h_n\}$ is the sequence of positive bandwidth such that $h_n \to 0$ and $nh_n \to \infty$ as $n \to \infty$. Here, K is a non negative kernel satisfying $\int K(x)dx = 1$, $\int K^2(x)dx < \infty$, and the kernel is assumed to have a compact support $[-\tau, \tau]$, for some $\tau > 0$. Suppose the covariates $\{x_i : i = 1, \ldots, n\}$ lie in a compact interval $[0, 1]$ (all the results are valid for any specified interval $[a, b]$ as well, where $a \in \mathbb{R}$ and $b \in \mathbb{R}$), and $s_1, s_2, ...s_n$ are such that, $0 < s_1 \leqslant s_2 \leqslant ... \leqslant s_n < 1$, with $x_j \leqslant s_j \leqslant x_{j+1}$, for all $j = 1, \ldots, n$, and $\max_j |s_j - s_{j-1}| = O\left(\frac{1}{n}\right)$.

In the spirit of Gasser-Muller estimator, one can estimate the $(r-1)$-th order derivative of the regression function as follows:

$$\hat{m}_{n,r-1}(t) = \frac{1}{h_n^r} \sum_{j=1}^{n} y_j \int_{s_{j-1}}^{s_j} K^{(r-1)}\left(\frac{t-u}{h_n}\right) du. \tag{2}$$

Here $K^{(r-1)}$ denotes the $(r-1)$-th order derivative of a $(r-1)$ times differentiable kernel function K with support $[-\tau, \tau]$ satisfying $\int_{-\tau}^{\tau} K(x)dx = 1$ and $K^{(j)}(-\tau) = K^{(j)}(\tau) = 0$, for all $j = 0, 1, \ldots r-1$, and $t \in [0, 1]$. *Here it should be pointed out that the randomness of the derivative estimator $\hat{m}_{n,r-1}(t)$ is obtained through ϵ_j involved in y_j for $j = 1, \ldots, n$.*

Motivated by the aforementioned facts, we propose a process, which is the key compo-

nent of our graphical device.

$$A_{n,r}(t) = \frac{2}{n(n-1)} \sum_{1 \leqslant k \neq i \leqslant n} sign\left\{\left(\hat{m}_{n,r-1}(x_i) - \hat{m}_{n,r-1}(x_k)\right)(x_i - x_k)\right\} \times k_n(x_i - t) \times k_n(x_k - t), \tag{3}$$

where $k_n(u) = \frac{1}{h_n} K\left(\frac{u}{h_n}\right)$. Note that the above process involves the product of two kernel functions evaluated at x_i and x_k to incorporate the local effect of the observation x_i and x_k. Theorem 2.1 gives us an insight about the behaviour of this process when the null hypothesis is true and the assertion described in the theorem will be the crux of our graphical device. Before proceeding to the main theorem, we state the assumptions required for the technicalities :

(A1) The observations on the covariates, i.e., x_i, $i = 1, \ldots, n$, are lying in the interval $[0, 1]$, even though any other closed interval can be considered. Moreover, $E(\epsilon) = 0$ and $E(\epsilon^2) < \infty$.

(A2) The nonparametric regression function $m(\cdot)$ is $(r+1)$ times continuously differentiable on the compact interval $[0, 1]$.

(A3) The sequence of positive bandwidth $\{h_n\}$ satisfies, $h_n \to 0$ and $nh_n^{2r+1} \to \infty$ as $n \to \infty$.

(A4) The kernel function K is continuous, and it is supported on $[-\tau, \tau]$, with $\int_{-\tau}^{\tau} K(x)dx = 1$.

(A5) Let $s_1, s_2, \ldots, s_n$ be a partition of $[0, 1]$ such that, $0 < s_1 \leqslant s_2 \leqslant \ldots \leqslant s_n < 1$, with $x_j \leqslant s_j \leqslant x_{j+1}$, $j = 1, \ldots, n$, and $\max_j |s_j - s_{j-1}| = O\left(\frac{1}{n}\right)$.

(A6) The kernel K is $(r+1)$ times continuously differentiable function satisfying $K^{(j)}(-\tau) = K^{(j)}(\tau) = 0$, for all $j = 0, 1, \ldots r$.

The assumption (A1) requires that the covariates lie in a closed interval. We need the interval to be closed for boundedness of estimators, required in the proof of Theorem 2.1.

Also, to use the Gasser-Muller derivative estimator, we require $E(\epsilon^2) < \infty$. Assumption (A2) is required in the proof of Theorem 2.1, for boundedness of $(r+1)$-th order derivative estimator of regression function. Assumption (A3) is a standard assumption for consistency of r-th order derivative estimator. To define the Gasser-Muller derivative estimator, we also need assumptions (A4) and (A5). Finally, (A6) is required for $(r+1)$-th order derivative estimator to be defined and bounded.

Theorem 2.1. *Under the assumptions (A1) - (A6), we have*

$$m^{(r)}(t) > 0 \,(\textit{i.e., when}\, H_0 \,\textit{is true}) \quad \textit{iff} \quad \liminf_n \inf_t A_{n,r}(t) > 0 \ \textit{with probability 1,}$$

where $m^{(r)}(\cdot)$ is the r-th order derivative of the regression function, $A_{n,r}(t)$ is as defined in (3), and r is a positive integer.

Construction of Graphical Device: The assertion in Theorem 2.1 implies that $A_{n,r}(t)$ is greater than zero for $t \in [0,1]$, if the null hypothesis is true. This fact inspires us to propose a graphical device based on $A_{n,r}(t)$ to check whether the r-th order derivative of the regression function is positive or not. In fact, on a lighter note, non-negative case can also be included in practice. *To summarize, our graphical device plots $A_{n,r}(t)$ for different values of t, and one needs to check whether the points of the set $\{(t, A_{n,r}(t)) : t \in [0,1]\}$ lie above the x-axis or not. In other words, the plotting of the points in the aforementioned set is our proposed graphical device.* The next section presents examples to illustrate how the graphical device works. We end this section with a remark on the proposed graphical device and a motivating example.

Remark 2.2. *For a given data, we may use a scatter plot to visualize the relationship between y and x. However, for any non-trivial relationship between y and x, the scatter plot may not reveal the true picture. In contrast, our graphical device can characterize the relationship between y and x by simply observing whether the points of our graphical device are clustering above the x-axis or not.*

A motivating example: To support the claim in Remark 1, let us consider a model $y = exp(x) + \epsilon$, where the error ϵ follows a standard Cauchy distribution. Note that

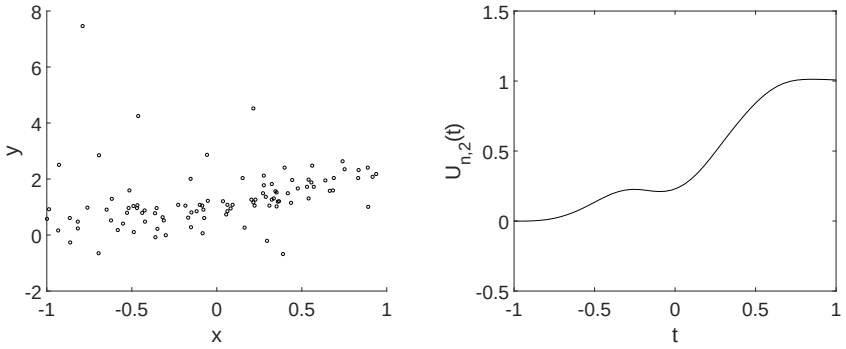

Figure 1: Scatter plot of $y = exp(x) + \epsilon$ (Left), and plot of $A_{n,2}(t)$ (Right) for different values of t.

$exp(x)$ is a strictly convex function of x. However, due to the presence of a few outliers generated by the Cauchy distribution, the scatter plot of (x, y) presented in the left panel of Figure 1 does not reveal the inherent feature of the functional relationship between x and y. Nevertheless, the plot of $A_{n,2}(t)$ with respect to t in the right panel of Figure 1, amply indicates the convex relationship between x and y. This example drives us to further investigate the proposed graphical device.

2.1 Examples for Illustration of the Graphical Device

In this section, we consider a few examples to demonstrate the working of our graphical device. At first, we consider a few convex functions, and plot $A_{n,2}(t)$ based on the second derivative (second derivative of the convex function is non-negative). The observations of the covariate are five hundred fixed values in $[-1, 1]$. The errors are generated from a Gaussian distribution with mean 0 and standard deviation 0.1. The Cosine kernel which is defined as $K(u) = \frac{\pi}{4}\cos\left(\frac{\pi}{2}u\right)$ with support $\{|u| \leqslant 1\}$, is used in the examples 1 to 10 below with $n = 500$.

Example 1: $m(x) = x^2$, **Example 2:** $m(x) = x^4$,

Example 3: $m(x) = e^x$, **Example 4:** $m(x) = \sin\left(\frac{\pi}{2}x\right)$.

As expected, the four panels in Figure 2 present the plots of $A_{n,2}(t)$ which shows that all points lie above the horizontal axis since the functions are convex function.

We now consider four examples of concave functions:

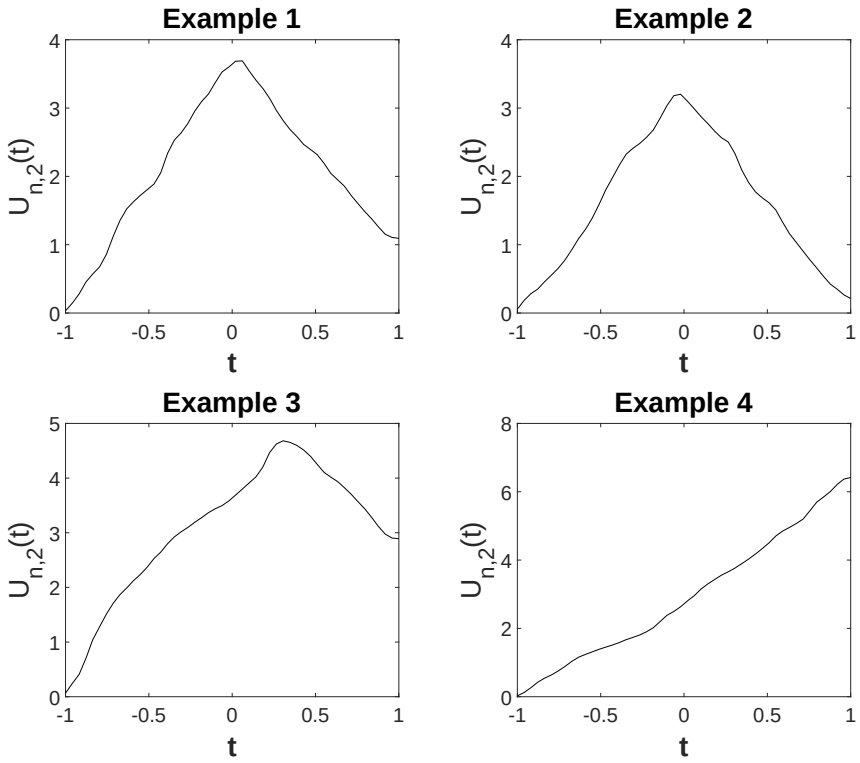

Figure 2: Plot of $A_{n,2}(t)$ for different values of t, for Examples 1, 2, 3 and 4.

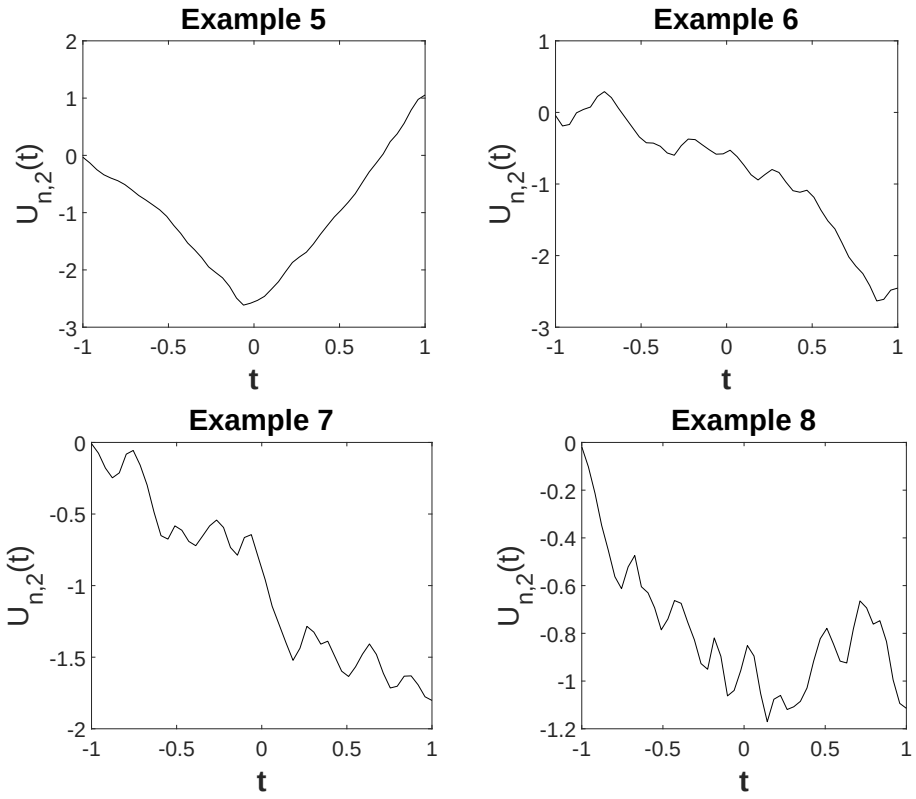

Figure 3: Plot of $A_{n,2}(t)$ for different values of t for Examples 5, 6, 7 and 8.

Example 5: $m(x) = -x^2$, **Example 6**: $m(x) = -e^x$,

Example 7: $m(x) = e^{-x^2}$, **Example 8**: $m(x) = \cos x$.

Figure 3 illustrates the diagrams, and here also, $n = 500$ is considered. For these examples, as expected, the points are clustered below the horizontal axis.

Finally, to examine the performance of our graphical device associated with higher order derivatives, we consider the following examples:

Example 9: $m(x) = x^4 - 4x^3 + 6x^2 + 1$, **Example 10**: $m(x) = -x^4 + 4x^3 - 6x^2 + 1$.

Note that the polynomial mentioned in Example 9 has positive third derivative, whereas Example 10 has negative third derivative. Figure 4 illustrates the diagrams when $n = 500$. As expected, the points in the graph for Example 9 lie above the horizontal axis, while for Example 10, the points lie below the horizontal axis. Overall, this study demonstrates the practical utility of the proposed graphical device to detect complex shapes of unknown

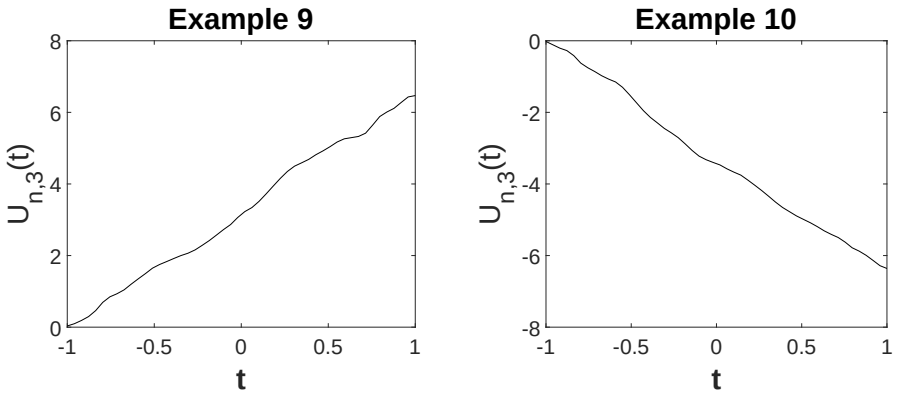

Figure 4: Plot of $A_{n,3}(t)$ for different values of t for Examples 9 and 10.

regression functions.

3 Tests for Derivatives of Regression Function

In Section 2, we showed that $\liminf_n \inf_t A_{n,r}(t) > 0$ is an equivalent condition for the null hypothesis to be true. This drives us to use an appropriate difference between the graph of $A_{n,r}(t)$ and the horizontal axis to carry out a formal test. In other words, we want to measure the extent to which $A_{n,r}(t)$ deviates from the horizontal axis when the null hypothesis is true. To develop a formal test, we require a proper normalization of $A_{n,r}(t)$ so that the final form $M\left(\sqrt{nh_n}\,[A_{n,r}(t) - E_{H_0}A_{n,r}(t)]\right)$ can be used for testing, where $M : C[0,1] \to \mathbb{R}_+$ is a positive functional, and $C[0,1]$ denotes the class of continuous functions defined over $[0,1]$. Two special choices of M lead to well known measures of discrepancy. Let $M_1(f) = \sup_{t\in[0,1]} |f(t)|$ and $M_2(f) = \int_0^1 f^2(t)\,dt$, then the corresponding test statistics are $T_{n,1} = \sup_{t\in[0,1]} \sqrt{nh_n}\,|(A_{n,r}(t) - E_{H_0}A_{n,r}(t))|$ and $T_{n,2} = nh_n \int_0^1 (A_{n,r}(t) - E_{H_0}A_{n,r}(t))^2\,dt$. In the numerical study presented later, the tests based on $T_{n,1}$ and $T_{n,2}$ are considered. However, in principle, one may consider tests based on other test statistics obtained by various choices of M. Theorem 3.1 describes the asymptotic distribution of $M\left(\sqrt{n}\,[A_{n,r}(t) - E_{H_0}A_{n,r}(t)]\right)$.

Theorem 3.1. *Under (A1) - (A6), we have*

$$\sup_{t\in[0,1]} \left| M\left(\sqrt{nh_n}\left[A_{n,r}(t) - E[A_{n,r}(t)]\right]\right) - M(G_n(t))\right| \xrightarrow{p} 0$$

as $n \to \infty$, where $M : C[0,1] \to \mathbb{R}$, $G_n(t)$ is a Gaussian process having $E[G_n(t)] = 0$, and for $t_1 \neq t_2$,

$$E\left[G_n(t_1)G_n(t_2)\right] = \int K(u)K\left(u + \frac{t_1 - t_2}{h_n}\right)\theta(t_1,t_1)\theta(t_1,t_2)f_{X_1}(u)du,$$

where $\theta(u,v) = \int sign\left\{\left(m^{(r-1)}(u) - m^{(r-1)}(z)\right)(u-z)\right\}k_n(z-v)f_{X_2}(z)dz$.

The proof of Theorem 3.1 utilizes Lemma 5.5 and Lemma 5.6 presented in the Appendix along with their proofs. The assertion of Lemma 5.5 essentially shows that a close approximation of $A_{n,r}(t)$ (denoted by $B_{n,r}(t)$) converges weakly to a certain Gaussian process after appropriate normalization, and Lemma 5.6 asserts that the uniform difference between $A_{n,r}(t)$ and $B_{n,r}(t)$ is negligible at a certain order. Finally, an application of Slutsky's theorem (see Serfling (2009)) completes the proof of Theorem 3.1.

The asymptotic distributions of $T_{n,1}$ and $T_{n,2}$ directly follows from Theorem 3.1. For sake of completeness, the statement for the asymptotic distributions are stated as a corollary below:

Corollary 3.2. *Under assumptions (A1) - (A6), we have*

$$T_{n,1} - \sup_{t\in[0,1]} |G_n(t)| \xrightarrow{p} 0 \text{ as } n \to \infty, \text{ and } T_{n,2} - \int_0^1 G_n^2(t)\,dt \xrightarrow{p} 0 \text{ as } n \to \infty,$$

where $T_{n,1} = \sup_{t\in[0,1]} \sqrt{nh_n}\,|(A_{n,r}(t) - E_{H_0}A_{n,r}(t))|$, $T_{n,2} = nh_n \int_0^1 (A_{n,r}(t) - E_{H_0}A_{n,r}(t))^2\,dt$, and $G_n(t)$ is a Gaussian process satisfying the same properties as in Theorem 3.1.

Next we describe how to carry out the test based on $T_{n,1}$ only. The test based on $T_{n,2}$ (or $M(\cdot)$) can be performed similarly, but not described for the sake of brevity. To implement the test based on $T_{n,1}$, we need to compute the quantile of the distribution of $\sup_{t\in[0,1]} |G(t)|$.

This is typically intractable, and so, we approximate the Gaussian process $G(t)$ by an appropriate large dimensional multivariate normal distribution and generate a sufficiently large data. The critical value at α level of significance can be estimated by the $(1-\alpha)$-th quantile of the large data. In order to estimate the power, one can generate a large data from the alternative model with a large number of replications, and the estimated power will be the proportion of times the value of test statistic exceeds the estimated critical value.

3.1 Finite Sample Power Study

In Section 3, we established the asymptotic distribution of $M(\cdot)$, and it directly follows from Theorem 3.1 that the test based on $M(\cdot)$ will be consistent, i.e., under fixed alternative hypothesis, the power of the test will converge to one as the sample size tends to infinity. Since $T_{n,1}$ and $T_{n,2}$ are obtained as special cases of M, i.e., when $M = M_1$ and $M = M_2$ respectively, the tests based on $T_{n,1}$ and $T_{n,2}$ will also be consistent. Having established the consistency property of the tests, it is of interest to see the performance of the tests when the sample size is finite. This is investigated below.

The expression $E_{H_0}[A_{n,r}(t)]$ present in the asymptotic result may be difficult to compute for a given data. To overcome this issue, we estimate $E[A_{n,r}(t)]$ by $g_n(t)$, which is given by $g_n(t) = \frac{1}{n^2} \sum_{1 \leqslant i \neq k \leqslant n} \frac{1}{h_n} K\left(\frac{x_i - t}{h_n}\right) \frac{1}{h_n} K\left(\frac{x_k - t}{h_n}\right)$. Note that $\sup_{t \in [0,1]} \sqrt{nh_n}\, |g_n(t) - E_{H_0}[A_{n,r}(t)]| \to 0$ almost surely as $n \to \infty$ (see Lemma 5.7 in the Appendix).

We now consider the following two examples:

Example 11: Under H_0, $m(x) = x^2$ and under H_1, $m(x) = -x^2$.

Example 12: Under H_0, $m(x) = e^x$ and under H_1, $m(x) = -e^x$.

In both the examples, $m(x)$ is a convex function of x under the null hypothesis (i.e., H_0), and $m(x)$ is a concave function of x under under the alternative hypothesis (i.e., H_1). As we know, the second derivative of any convex function is non-negative, we investigate power properties of tests when $v = 2$. For concise presentation, we study only the tests based on $T_{n,1}$ and $T_{n,2}$. However, in principle, one may consider other functional forms as mentioned

Sample Size ↓	**Example 11.** H_0: $\mu(x) = x^2$, H_1: $\mu(x) = -x^2$		**Example 12.** H_0: $\mu(x) = e^x$, H_1: $\mu(x) = -e^x$	
	Power of $T_{n,1}$	Power of $T_{n,2}$	Power of $T_{n,1}$	Power of $T_{n,2}$
50	0.0533	0.0133	0.0780	0.0267
100	0.2933	0.2800	0.128	0.1600
200	0.7840	0.9804	0.3922	0.8431
300	0.9020	1.0000	0.4902	0.952
400	0.9412	1.0000	0.7440	1.0000
500	0.9608	1.0000	0.9437	1.0000

Table 1: The estimated power of the tests $T_{n,1}$ and $T_{n,2}$ in case of Example 11 and 12, for different sample sizes.

earlier.

To implement the tests, we compute the critical value (denoted as c_α) following the procedure described in the last paragraph of Section 3. To compute the finite sample power, we generate $N(=150)$ observations from the model defined for the alternative hypothesis (denote those observations as $D_1, \ldots, D_N$) and compute the value of the test statistic for $D_1, \ldots, D_N$. Let $t_1, \ldots, t_N$ denote the values of the test statistics, and finally, at $(1-\alpha)\%$ level of significance, the finite sample power is estimated as the proportion of times $t_1, \ldots, t_N$ exceeding c_α. The estimated power of the tests are presented in Table 1, and the finite sample power is depicted in Figure 5 for different values of n. Similar to the examples in Section 2, we have considered Cosine kernel.

The values in Table 1 and the power curve of Figure 5 indicate that the power of both the tests increases as the sample size increases, and it concurs with expectation since both the tests are consistent. Also, the tests based on $T_{n,1}$ and $T_{n,2}$ are reasonably powerful, even for small sample sizes.

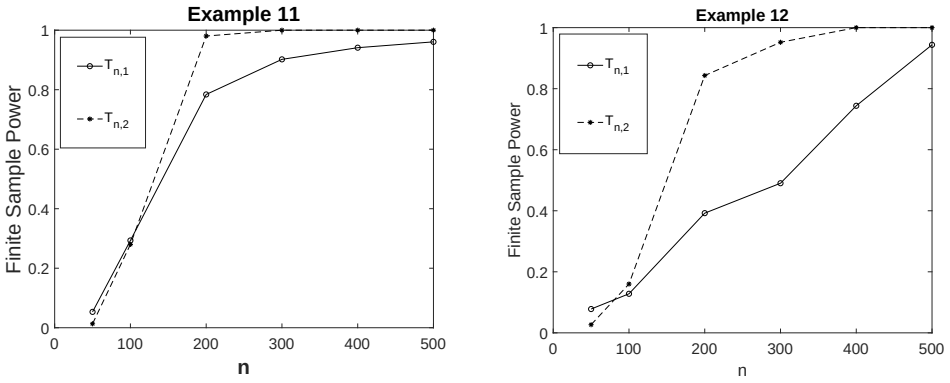

Figure 5: Plot of Finite Sample Power of Example 11 and 12 for different sample sizes.

3.2 Real Data Analysis

This section implements the graphical device on multiple real data examples collected from Ruppert, Wand, and Carroll (2003) and UCI Machine Learning Repository. A description of all the data are presented below, and Cosine kernel is used as in the simulation study.

Real Data 1 (Onion Growth): We first consider the onion growth data from Section 7.2 of the book by Ruppert et al. (2003), which was studied in the context of the production of white Spanish onions in two South Australian locations. This data can be accessed through the link: `http://matt-wand.utsacademics.info/webspr/onions.txt`. The data has three variables, namely, onion yield (in grammes per plant), areal density of plants (in plants per square metre) and location (0 = Purnong Landing, 1 = Virginia). We consider only two variables, i.e., 'areal density of plants' as independent variable and 'onion yield' as dependent variable. The data contains 84 observations for onion yield with respect to different areal density of plants. We first look at the scatter plot of the data (left panel of Figure 6) which reveals that the unknown relationship between the dependent and the independent variables may be approximated by a convex function.

In order to verify whether the unknown relationship can be described by a convex function, we plot $A_{n,2}(t)$ based on the second order derivative for different values of t and observe that all points in the plot of $A_{n,2}(t)$ lie above the horizontal axis (right panel in Figure 6). This pictorial representation gives a clear insight that the unknown relationship for this real data is convex in nature. The p-value, computed by re-sampling this data 120

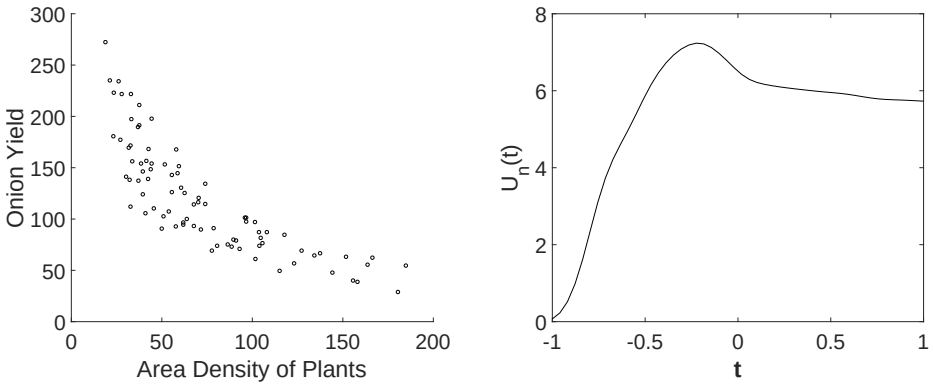

Figure 6: Scatter plot of onion growth data (left) and plot of $A_{n,2}(t)$ for different values of t for the same data (right).

times, comes out to be 0.4681 in case of $T_{n,1}$ and 0.3478 in case of $T_{n,2}$.

Real Data 2 (LIDAR): We next consider Light Detection and Ranging data (LIDAR) from Section 2.7 of Ruppert et al. (2003). This data can be accessed through the link: `http://matt-wand.utsacademics.info/webspr/lidar.txt`. The data has two variables, namely, 'distance travelled before the light is reflected to its source' and 'logarithm of the ratio of received light from two laser sources'. There are 221 observations from LIDAR experiment. We consider distance travelled as independent variable, and logarithm of the ratio as dependent variable. We look at the scatter plot of the data (left panel of Figure 7), which indicates that the points are clustered in a concave-like shape. The plot of $A_{n,2}(t)$ is presented in the right panel of Figure 7, and all points of the plot lie below the horizontal axis. In other words, it gives us an impression that the two variables of this real data has a concave functional relationship. The p-values computed by re-sampling is very close to zero for both $T_{n,1}$ and $T_{n,2}$, which further supports the fact that the data does not represent convex shape.

Real Data 3 (Fossil Shells): We consider the fossil shell data from strontium-isotope stratigraphy of deep-sea sections, analyzed in Section 3.6 of Ruppert et al. (2003). This data can be accessed through the link: `http://matt-wand.utsacademics.info/webspr/fossil.txt`. The data has two variables, namely, 'age in millions of years of fossil shells' and 'ratios of strontium isotopes'. The independent variable under consideration is 'age', and the 'ratio'

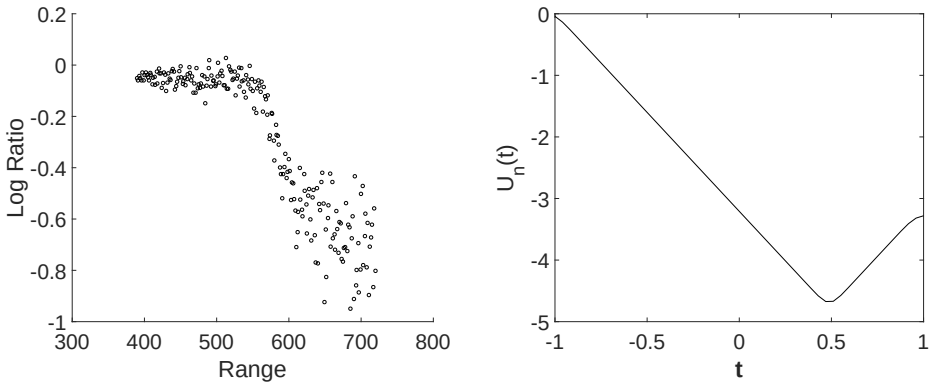

Figure 7: Scatter plot of LIDAR data (left) and plot of $A_{n,2}(t)$ for different values of t for the same data (right).

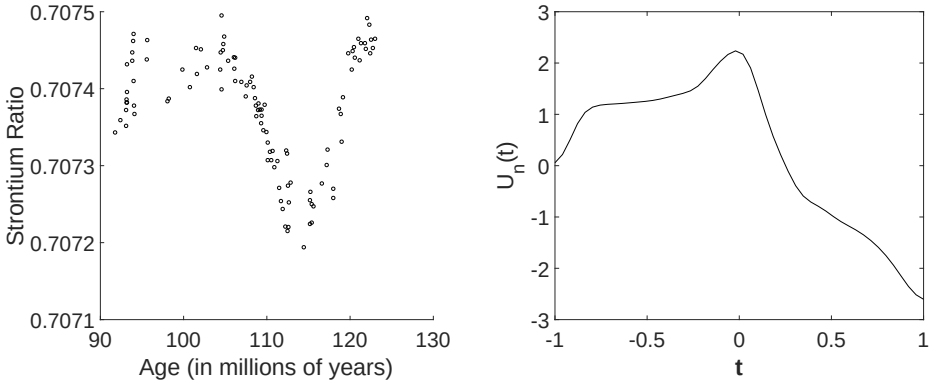

Figure 8: Scatter plot of Fossil Shell data (left) and plot of $A_{n,2}(t)$ for different values of t for the same data (right).

is considered as dependent variable. We first present a scatter plot of the data (left panel of Figure 8), which shows that the relationship is convex in some parts and concave in other parts. Similar inference can be drawn from the plot of $A_{n,2}(t)$ presented in the right panel of Figure 8, where points are clustered on both sides of the horizontal line ($t = 0$). It is worth noting that, the points in the plot of $A_{n,2}(t)$ has more clustering on the positive side, because the data shows convex shaped clustering in major parts of the plot. Here, the p-value after re-sampling is 0.0010 for $T_{n,1}$ and 0.0238 for $T_{n,2}$, which indicates that the unknown function is not convex.

Real Data 4 (Yacht Hydrodynamics): Finally, we consider yacht hydrodynam-

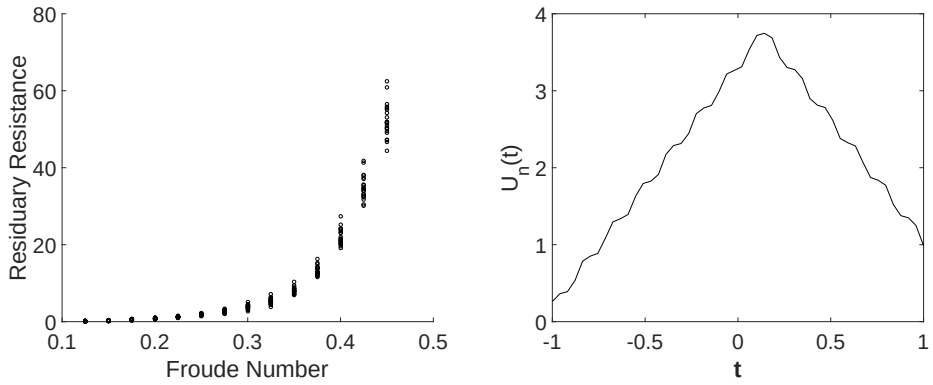

Figure 9: Scatter plot of Yacht Hydrodynamics data (left) and plot of $A_{n,2}(t)$ for different values of t for the same data (right).

ics data from `https://archive.ics.uci.edu/ml/datasets/Yacht+Hydrodynamics`. The data has seven attributes, but we only consider two variables: 'Froude Number' as independent variable, and 'Residuary resistance per unit weight of displacement' as the dependent variable. We display the scatter plot of the data in the left panel of Figure 9, which shows a convex functional curve. The plot of $A_{n,2}(t)$ is presented in the right panel of Figure 9, which shows that all points are above the horizontal axis as expected. Finally, the p-value using re-sampling comes out to be 0.3750 for $T_{n,1}$ and 0.3438 for $T_{n,2}$ which also stipulates that the unknown function is convex.

4 Concluding Remarks

In this article, we propose a new graphical device based on a certain process and show that it can be used to check whether the derivative of regression function of a particular order is positive or not, i.e., in other words, it gives us insight about the shape of the regression function. Non-technically speaking, the points of our graphical device will be clustered above the horizontal axis when the certain order of derivative is positive, which is a necessary and sufficient condition. We illustrate the plots of our graphical device in multiple studies, and they reveal that the proposed graphical device can correctly identify the feature of the unknown regression function. We further investigate the aforementioned

problem based on a class of test statistics; in particular the performance of the tests based on $T_{n,1}$ and $T_{n,2}$– test statistics defined with respect to supremum norm and $\mathcal{L}_2$ norm, respectively. Besides, we implement our graphical device in several real data examples, and observe that the graphical device is able to correctly identify the feature of the real data.

In the context of hypothesis testing, we only discuss the tests based on $T_{n,1}$ and $T_{n,2}$. However, in principle different choices of functional M will give us different choices of test statistics. In future, one may have interest to see the performance of the tests based on other test statistics obtained by different choices of M.

The choices of the kernel and the bandwidth are another issues of concern. In fact, different choices of those may produce different results. We here choose the kernel and the bandwidth such a way so that the conditions on those are satisfied. However, there is no guarantee that any other choice will not produce better result. Besides, one may also select the bandwidth using data driven approach; it however will make the procedure theoretically more challenging.

Acknowledgement

The idea of the problem discussed in the article came to the first author's mind while he was visiting The Michigan State University, USA, during the academic session 2015-2016. The first author would like to thank Prof. Hira Koul for many innovative suggestions on the proposed graphical device and Theorem 2.1. The second author is thankful to the Council of Scientific and Industrial Research, India for his PhD fellowship. The authors are thankful to Mr. Pranay Tarafdar for his initial involvement with this work.

5 Appendix

Proof of Theorem 2.1 and Supporting Lemmas

We need the following lemmas in the proof of Theorem 2.1:

Lemma 5.1. *Let m be r times differentiable (for $r = 0$, m is continuous), and $K^{(r)}$ (i.e., r-th order derivative of K) is bounded. Then $\hat{m}_{n,r}(t)$ is a strongly consistent estimate of $m^{(r)}(t)$ if*

(a) $m^{(r)}$ is continuous at t, and

(b) $n\,h_n^{2r+1} \to \infty$ and $h_n \to 0$ as $n \to \infty$.

Proof. See the proof of Theorem 1 in Gasser and Müller (1984). □

Lemma 5.2. *Let m be r times differentiable, $K^{(r)}$ be bounded, and $m^{(r)}$ be continuous at t. Then*

$$\sup_{t\in[0,1]} E\left(\left|\hat{m}_{n,r}(t) - m^{(r)}(t)\right|^2\right) \longrightarrow 0$$

as $n \to \infty$, for a fixed positive integer r, where $\{h_n\}$ is a sequence of positive bandwidth such that $n\,h_n^{2r+1} \to \infty$, $h_n \to 0$ as $n \to \infty$, and $[0,1]$ is the interval containing all the covariates inside the domain of definition of regression function m.

Proof. See the proof of Theorem 1, in Georgiev (1984). □

Lemma 5.3. *Consider sequences of functions $f_n(t)$ and $g_n(t)$ defined on an interval $[a,b]$ such that $f_n(t) \to f(t)\,(> 0)$ uniformly (for $t \in [a,b]$) and $g_n(t) \to 0$ uniformly (for $t \in [a,b]$) as $n \to \infty$, then*

$$sign\{f_n(t) + g_n(t)\} \longrightarrow sign\{f(t)\} \text{ uniformly over } t \in [a,b].$$

Proof. Since $f(t) > 0$, for a positive $\epsilon < \inf_t f(t)$, there exists an N_1 such that,

$$\sup_{t\in[a,b]} |f_n(t) - f(t)| < \frac{\epsilon}{2}, \qquad \text{for all} \quad n > N_1. \tag{4}$$

Also note that, since $g_n(t) \to 0$ as $n \to \infty$ uniformly, for the same ϵ there exists an N_2 such that,

$$\sup_{t\in[a,b]} |g_n(t) - 0| < \frac{\epsilon}{2}, \qquad \text{for all} \quad n > N_2.$$

We can infer that for all $n > N(= \max\{N_1, N_2\})$,

$$\sup_{t\in[a,b]} |f_n(t) + g_n(t) - f(t)| \leqslant \sup_{t\in[a,b]} |f_n(t) - f(t)| + \sup_{t\in[a,b]} |g_n(t)| < \epsilon < \inf_{t\in[a,b]} f(t).$$

The above inequality implies that $f_n(t) + g_n(t) > 0$ for all $n > N$, which in turn implies that $sign\{f_n(t) + g_n(t)\} = 1 = sign\{f(t)\}$ for all $n > N$. This completes the proof. □

Proof of Theorem 2.1:

Proof. Consider the process defined in (3), i.e., $A_{n,r}(t)$ for $t \in [0, 1]$ with the derivative estimator of the regression function proposed in Gasser and Müller (1984).

$$\begin{aligned}
A_{n,r}(t) &= \frac{1}{n(n-1)} \sum_{1\leq k\neq i\leq n} sign\left\{(\hat{m}_{n,r-1}(x_i) - \hat{m}_{n,r-1}(x_k))\,(x_i - x_k)\right\} \\
&\quad \times k_n(x_i - t)k_n(x_k - t) \\
&= \frac{1}{n(n-1)} \sum_{1\leq k\neq i\leq n} sign\Bigg\{ (x_i - x_k) \left(\frac{1}{h_n^r} \sum_{j=1}^{n} y_j \int_{s_{j-1}}^{s_j} K_{r-1}\left(\frac{x_i - u}{h_n}\right) du \right. \\
&\quad \left. - \frac{1}{h_n^r} \sum_{j=1}^{n} y_j \int_{s_{j-1}}^{s_j} K_{r-1}\left(\frac{x_k - u}{h_n}\right) du \right) \Bigg\} \times k_n(x_i - t)k_n(x_k - t) \\
&= \frac{1}{n(n-1)} \sum_{1\leq k\neq i\leq n} sign\Bigg\{ (x_i - x_k) \frac{1}{h_n^r} \sum_{j=1}^{n} y_j \int_{s_{j-1}}^{s_j} \left(K_{r-1}\left(\frac{x_i - u}{h_n}\right) \right. \\
&\quad \left. - K_{r-1}\left(\frac{x_k - u}{h_n}\right) \right) du \Bigg\} \times k_n(x_i - t)k_n(x_k - t),
\end{aligned} \tag{5}$$

where $k_n(x_i - t) = \frac{1}{h_n} K\left(\frac{x_i - t}{h_n}\right)$. Under (A6), a Taylor series expansion of $K_{r-1}(\cdot)$ in the

neighbourhood of the point $\frac{t-u}{h_n}$ yields the following expression.

$$A_{n,r}(t) = \frac{1}{n(n-1)} \sum_{1\le k\neq i\le n} sign\Bigg\{(x_i - x_k)\frac{1}{h_n^r}\sum_{j=1}^{n} y_j \int_{s_{j-1}}^{s_j} \Bigg(K_{r-1}\left(\frac{t-u}{h_n}\right)$$
$$+ \frac{(x_i-t)}{h_n}K_r\left(\frac{t-u}{h_n}\right) + \frac{1}{2!}\frac{(x_i-t)^2}{h_n^2}K_{r+1}\left(\frac{\xi_i-u}{h_n}\right) - K_{r-1}\left(\frac{t-u}{h_n}\right)$$
$$- \frac{(x_k-t)}{h_n}K_r\left(\frac{t-u}{h_n}\right) - \frac{1}{2!}\frac{(x_k-t)^2}{h_n^2}K_{r+1}\left(\frac{\xi_k-u}{h_n}\right)\Bigg)du\Bigg\}k_n(x_i-t)k_n(x_k-t),$$

where $\xi_i \in (x_i, t)$ and $\xi_k \in (x_k, t)$, for all $i, k = 1, 2, \ldots, n$. Accumulating the similar terms, we obtain

$$A_{n,r}(t) = \frac{1}{n(n-1)} \sum_{1\le k\neq i\le n} sign\Bigg\{(x_i - x_k)\frac{1}{h_n^r}\sum_{j=1}^{n} y_j \int_{s_{j-1}}^{s_j} \Bigg(\frac{(x_i-x_k)}{h_n}K_v\left(\frac{t-u}{h_n}\right) +$$
$$\frac{(x_i-t)^2}{2h_n^2}K_{r+1}\left(\frac{\xi_i-u}{h_n}\right) - \frac{(x_k-t)^2}{2h_n^2}K_{r+1}\left(\frac{\xi_k-u}{h_n}\right)\Bigg)du\Bigg\}k_n(x_i-t)k_n(x_k-t),$$

Simplifying the expression, we have,

$$\begin{aligned} A_{n,r}(t) = \frac{1}{n(n-1)} \sum_{1\le k\neq i\le n} sign\Bigg\{ & (x_i - x_k)^2\frac{1}{h_n^{r+1}}\sum_{j=1}^{n} y_j \int_{s_{j-1}}^{s_j} K_v\left(\frac{t-u}{h_n}\right)du \\ & + (x_i - x_k)\frac{(x_i-t)^2}{2}\frac{1}{h_n^{r+2}}\sum_{j=1}^{n} y_j \int_{s_{j-1}}^{s_j} K_{r+1}\left(\frac{\xi_i-u}{h_n}\right)du \\ & - (x_i - x_k)\frac{(x_k-t)^2}{2}\frac{1}{h_n^{r+2}}\sum_{j=1}^{n} y_j \int_{s_{j-1}}^{s_j} K_{r+1}\left(\frac{\xi_k-u}{h_n}\right)du\Bigg\} \\ & \times k_n(x_i-t)k_n(x_k-t) \end{aligned}$$

Further simplifying the expression in terms of $\hat{m}_{n,r}$ provides us,

$$\begin{aligned} A_{n,r}(t) &= \frac{1}{n(n-1)} \sum_{1\leq k\neq i\leq n} sign\Big\{(x_i-x_k)^2\hat{m}_{n,r}(t)+ \\ &\quad (x_i-x_k)\frac{(x_i-t)^2}{2}\hat{m}_{n,r+1}(\xi_i) - (x_i-x_k)\frac{(x_k-t)^2}{2}\hat{m}_{n,r+1}(\xi_k)\Big\} \\ &\quad \times k_n(x_i-t)k_n(x_k-t) \qquad (6) \\ &= \frac{1}{n(n-1)} \sum_{1\leq k\neq i\leq n} sign\Big\{\hat{m}_{n,r}(t) + \frac{(x_i-t)^2}{2(x_i-x_k)}\hat{m}_{n,r+1}(\xi_i) \\ &\quad - \frac{(x_k-t)^2}{2(x_i-x_k)}\hat{m}_{n,r+1}(\xi_k)\Big\} \times k_n(x_i-t)k_n(x_k-t). \end{aligned}$$

Following (A4), the support of kernel is the compact interval $[-\tau,\tau]$, and without loss of generality, we suppose that the support of kernel is $[-1,1]$. With this assumption, $k_n(x_i-t)$ is 0 outside the set $\left\{t\in[0,1]:\left|\frac{x_i-t}{h_n}\right|\leqslant 1\right\}$. Denote, $b_n(t) = \frac{(x_i-t)^2}{2(x_i-x_k)}\hat{m}_{n,r+1}(\xi_i)$ and $c_n(t) = \frac{(x_k-t)^2}{2(x_i-x_k)}\hat{m}_{n,r+1}(\xi_k)$, then $b_n(t), c_n(t) \to 0$ uniformly in probability as $h_n \to 0$, since $\hat{m}_{n,r+1}$ is bounded, following (A2) and (A6). Using Lemma 5.3 on $\hat{m}_{n,r}(t)$ and $b_n(t)-c_n(t)\to 0$ uniformly in probability as $n\to\infty$, we infer that for any $\epsilon>0$ there exists some positive integer N such that

$$\sup_{t\in[0,1]}\left|A_{n,r}(t) - \frac{sign\{m^{(r)}(t)\}}{n(n-1)}\sum_{1\leq k\neq i\leq n} k_n(x_i-t)k_n(x_k-t)\right| < \epsilon$$

for all $n>N$. Note that $t\mapsto k_n(x_i-t)$ is a non negative scaled kernel function for all $i=1,\ldots,n$, and hence $\frac{1}{n(n-1)}\sum_{1\leq k\neq i\leq n} k_n(x_i-t)k_n(x_k-t)$ is positive for all $t\in[0,1]$. Thus, we have $\inf_t A_{n,r}(t)>0$ for all $n>N$ if and only if $m^{(r)}(t)>0$, and hence,

$$\liminf_n \inf_{t\in[0,1]} A_{n,r}(t) > 0 \text{ with probability 1, if and only if } m^{(r)}(t)>0. \qquad (7)$$

□

Proof of Theorem 3.1 and Supporting Lemmas

Lemma 5.4. *Let*

$$B_{n,r}(t) = \frac{1}{n(n-1)} \sum_{1\le k\neq i\le n} sign\left\{\left(m^{(r-1)}(X_i) - m^{(r-1)}(X_k)\right)(X_i - X_k)\right\} \times k_n(X_i - t)k_n(X_k - t), \tag{8}$$

$$\theta(x_1) = \int sign\left\{\left(m^{(r-1)}(x_1) - m^{(r-1)}(z)\right)(x_1 - z)\right\} k_n(z - t) f_{X_2}(z)dz, \tag{9}$$

and $c_2 = \int\{K(u)\}^2 du$, *where* $m^{(r-1)}(\cdot)$ *is the* $(r-1)$*-th derivative of regression function* m *and* $k_n(\cdot)$ *is the scaled kernel function as defined in Section 2. Then we have,*

$$\sqrt{nh_n}\left(B_{n,r}(t_0) - E\left[B_{n,r}(t_0)\right]\right) \xrightarrow{d} \mathcal{N}(0, 4c_2\theta^2(t_0)f_{X_1}(t_0))$$

for a fixed t_0, *as* $n \to \infty$, *where* $f_{X_1}(\cdot)$ *is the probability density function of the random variable* X_1.

Proof. Let $\psi_{n,t_0}(x_1) = E\left[sign\left\{\left(m^{(r-1)}(X_1) - m^{(r-1)}(X_2)\right)(X_1 - X_2)\right\} k_n(X_1 - t_0)k_n(X_2 - t_0)|X_1 = x_1\right]$, and note that

$$\begin{aligned}
\psi_{n,t_0}(x_1) &= \int sign\left\{\left(m^{(r-1)}(x_1) - m^{(r-1)}(z)\right)(x_1 - z)\right\} k_n(x_1 - t_0)k_n(z - t_0)f_{X_2}(z)dz \\
&= k_n(x_1 - t_0)\int sign\left\{\left(m^{(r-1)}(x_1) - m^{(r-1)}(z)\right)(x_1 - z)\right\} k_n(z - t_0)f_{X_2}(z)dz \\
&= k_n(x_1 - t_0)\theta(x_1),
\end{aligned} \tag{10}$$

where $\theta(x_1) = \int sign\left\{\left(m^{(r-1)}(x_1) - m^{(r-1)}(z)\right)(x_1 - z)\right\} k_n(z - t_0)f_{X_2}(z)dz$. Now note that

$$\begin{aligned}
E\left[k_n(X_1 - t_0)\theta(X_1)\right] &= \int \frac{1}{h_n} K\left(\frac{x - t_0}{h_n}\right)\theta(x)f_{X_1}(x)dx \\
&= \int K(u)\theta(t_0 + h_n u)f_{X_1}(t_0 + h_n u)du,
\end{aligned}$$

using the transformation $u = \frac{x-t_0}{h_n}$. Now using Taylor expansion around the point t_0, we

have

$$E\left[k_n(X_1-t_0)\theta(X_1)\right] = f_{X_1}(t_0)\theta(t_0)\int K(u)du + h_n(f'_{X_1}(t_0)+\theta'(t_0))\int uK(u)du + O(h_n^2)$$
$$= f_{X_1}(t_0)\theta(t_0) + O(h_n^2). \tag{11}$$

Further, we have,

$$E\left[(k_n(X_1-t_0)\theta(X_1))^2\right] = \int \frac{1}{h_n^2}\left\{K\left(\frac{x-t_0}{h_n}\right)\theta(x)\right\}^2 f_{X_1}(x)dx$$
$$= \frac{1}{h_n}\int (K(u))^2\theta(t_0+h_nu)f_{X_1}(t_0+h_nu)du$$

using the transformation $u = \frac{x-t_0}{h_n}$. Now, we use Tailor expansion around the point t_0 to have

$$E\left[(k_n(X_1-t_0)\theta(X_1))^2\right] = \frac{1}{h_n}\int (K(u))^2(\theta^2(t_0)+O(h_n))(f_{X_1}(t_0)+O(h_n))du$$
$$= \frac{1}{h_n}c_2\theta^2(t_0)f_{X_1}(t_0) + O(1), \tag{12}$$

where $c_2 = \int\{K(u)\}^2du$. Combining (10), (11) and (12), we have (*var* denotes the variance)

$$var(\psi_{n,t_0}(x_1)) = \frac{1}{h_n}c_2\theta^2(t_0)f_{X_1}(t_0) + \{f_{X_1}(t_0)\theta(t_0)+O(h_n^2)\}^2 + O(1).$$

Note that for the fixed t_0, $B_{n,r}(t_0)$ is a U-statistic of order 2. Now, using the asymptotic distribution of U-statistics (see A. J. Lee (1990) for details) along with the fact that $h_n \to 0$ as $n \to \infty$, we have $\sqrt{nh_n}\left(B_{n,r}(t_0) - E\left[B_{n,r}(t_0)\right]\right) \xrightarrow{\mathrm{d}} \mathcal{N}(0, 4c_2\theta^2(t_0)f_{X_1}(t_0))$ as $n \to \infty$. It completes the proof. □

Lemma 5.5. *Let $B_{n,r}(t)$ be as defined in the statement of Lemma 5.4. Then*

$$\sup_{t\in[0,1]}\left|\sqrt{nh_n}\left[B_{n,r}(t) - E\left(B_{n,r}(t)\right)\right] - G_n(t)\right| \xrightarrow{P} 0, \text{ as } n \to \infty,$$

where $G_n(t)$ is same as defined in Theorem 3.1.

Proof. In order to prove this lemma, one needs to first establish that an arbitrary ordered finite dimensional distribution of $\sqrt{nh_n}[B_{n,r}(t) - E(B_{n,r}(t))]$ converges weakly to a certain multivariate normal distribution, and $\sqrt{nh_n}[B_{n,r}(t) - E(B_{n,r}(t))]$ is tight. Let us consider s (≥ 1) many arbitrary points $t_1, \ldots, t_s \in [0,1]$. Note that using Bahadur representation of U-statistic (see A. J. Lee (1990)), we have

$$B_{n,r}(t_i) - E[B_{n,r}(t_i)] = \frac{2}{n}\sum_{j=1}^{n} \tilde{\psi}_{n,t_i}(X_j) + R_n,$$

where $\tilde{\psi}_{n,t}(x) = \psi_{n,t}(x) - E[B_{n,r}(t)]$ and $\sqrt{n}R_n \xrightarrow{\text{P}} 0$ as $n \to \infty$. Here $\psi_{n,t}(\cdot)$ is same as defined in the proof of Lemma 5.4. This implies that,

$$\sum_{i=1}^{s} a_i \left(B_{n,r}(t_i) - E\left[B_{n,r}(t_i)\right]\right) = \frac{2}{n}\sum_{i=1}^{s} a_i \left(\sum_{j=1}^{n} \tilde{\psi}_{n,t_i}(X_j) + R_n\right).$$

Next, using Cramer-Wald device (see, Serfling (2009)) and Slutsky's theorem (see, Serfling (2009)), one can conclude that s-dimensional vector $\left(\sqrt{nh_n}[B_{n,r}(t_1) - E(B_{n,r}(t_1))], \ldots, \sqrt{nh_n}[B_{n,r}(t_s) - E(B_{n,r}(t_s))]\right)$ converges weakly to an s-dimensional multivariate normal distribution.

We now consider the expression $\sup_{t\in[0,1]} |B_{n,r}(t) - E[B_{n,r}(t)]|$. Note that

$$\begin{aligned} E[B_{n,r}(t)] &= E\left[sign\left\{\left(m^{(r-1)}(X_i) - m^{(r-1)}(X_k)\right)(X_i - X_k)\right\} k_n(X_i - t)k_n(X_k - t)\right] \\ &= \iint sign\left\{\left(m^{(r-1)}(u) - m^{(r-1)}(v)\right)(u - v)\right\} k_n(u - t)k_n(v - t)f_{X_1}(u)f_{X_1}(v)dudv. \end{aligned}$$

Hence,

$$\begin{aligned} |E[B_{n,r}(t)]| &\leqslant \left|\iint k_n(u - t)k_n(v - t)f_{X_1}(u)f_{X_1}(v)dudv\right| \\ &= \left(\int k_n(u - t)f_{X_1}(u)du\right)^2 = \left(\int K(z)f_{X_1}(t + h_n z)dz\right)^2, \end{aligned}$$

using the transformation $z = \frac{u-t}{h_n}$. Now, we use Tailor expansion of f_{X_1} around the point

t, to get

$$\int K(z) f_{X_1}(t + h_n z) dz = \int K(z)(f_{X_1}(t) + h_n z f'_{X_1}(t) + O(h_n^2)) dz = f_{X_1}(t) + O(h_n^2).$$

Hence,

$$|E[B_{n,r}(t)]| \leqslant f_{X_1}(t) + O(h_n^2). \tag{13}$$

Further,

$$\begin{aligned} |B_{n,r}(t)| &\leqslant \frac{1}{n(n-1)} \sum_{1 \leq k \neq i \leq n} \left| sign \left\{ \left(m^{(r-1)}(X_i) - m^{(r-1)}(X_k) \right) (X_i - X_k) \right\} k_n(X_i - t) k_n(X_k - t) \right| \\ &\leqslant \frac{1}{n(n-1)} \sum_{1 \leq k \neq i \leq n} \left| k_n(X_i - t) k_n(X_k - t) \right| \leqslant M^2, \end{aligned} \tag{14}$$

where $M = \limsup_n \sup_x k_n(x)$. Combining equations (13) and (14), we have $\sup_{t \in [0,1]} |B_{n,r}(t) - E(B_{n,r}(t))|$ is bounded in probability. The aforementioned two facts imply that $\sqrt{nh_n}[B_{n,r}(t) - E(B_{n,r}(t))]$, $t \in [0,1]$ converges weakly to a certain Gaussian process. Now, note that $E(\sqrt{nh_n}[B_{n,r}(t) - E(B_{n,r}(t))]) = 0$ and for any $t_1 \neq t_2$,

$$\begin{aligned} &Cov(\sqrt{nh_n}[B_{n,r}(t) - E(B_{n,r}(t_1))], \sqrt{nh_n}[B_{n,r}(t) - E(B_{n,r}(t_2))]) \\ &= E[\psi_{n,t_1}(X_1)\psi_{n,t_2}(X_1)] = E[k_n(X_1 - t_1)\theta(X_1, t_1)k_n(X_1 - t_2)\theta(X_1, t_2)] \\ &= \int k_n(x - t_1)\theta(x, t_1)k_n(x - t_2)\theta(x, t_2) f_{X_1}(x) dx \end{aligned}$$

Now, using the transformation $u = \frac{x - t_1}{h_n}$, we have

$$\begin{aligned} &Cov\left(\sqrt{nh_n}[B_{n,r}(t) - E(B_{n,r}(t_1))], \sqrt{nh_n}[B_{n,r}(t) - E(B_{n,r}(t_2))] \right) \\ &= \int K(u) \frac{1}{h_n} K\left(u + \frac{t_1 - t_2}{h_n} \right) \theta(t_1, t_1)\theta(t_2, t_2) f_{X_1}(u) du \end{aligned}$$

This implication follows from the fact that $h_n \to 0$ as $n \to \infty$ and an application of Dominated Convergence theorem (see, Billingsley (2008)). □

Lemma 5.6. *Let $A_{n,r}(t)$ be as defined in Section 2 and $B_{n,r}(t)$ be the same as defined in the*

statement of Lemma 5.4. Then we have, $\sup_{t\in[0,1]} \sqrt{nh_n}|A_{n,r}(t) - B_{n,r}(t)| \xrightarrow{P} 0$ *as* $n \to \infty$.

Proof. Note that

$$
\begin{aligned}
&\sup_{t\in[0,1]} \sqrt{nh_n}|A_{n,r}(t) - B_{n,r}(t)| \\
&\leqslant \sup_{t\in[0,1]} \frac{\sqrt{nh_n}}{n(n-1)} \sum_{1\leq k\neq i\leq n} \Big| sign\left\{\left(\hat{m}_{n,r-1}(X_i) - \hat{m}_{n,r-1}(X_k)\right)(X_i - X_k)\right\} \\
&- sign\left\{\left(m^{(r-1)}(X_i) - m^{(r-1)}(X_k)\right)(X_i - X_k)\right\} \Big| k_n(X_i - t)k_n(X_k - t) \\
&= \sup_{t\in[0,1]} \frac{\sqrt{nh_n}}{n(n-1)h_n^2} \sum_{1\leq k\neq i\leq n} \Big| sign\left\{\left(\hat{m}_{n,r-1}(X_i) - \hat{m}_{n,r-1}(X_k)\right)(X_i - X_k)\right\} \\
&- sign\left\{\left(m^{(r-1)}(X_i) - m^{(r-1)}(X_k)\right)(X_i - X_k)\right\} \Big| K\left(\frac{X_i - t}{h_n}\right) K\left(\frac{X_k - t}{h_n}\right)
\end{aligned}
$$

Since $\hat{m}_{r-1}(\cdot) \xrightarrow{\mathrm{P}} m^{(r-1)}(\cdot)$ uniformly as $n \to \infty$ (see, (Gasser & Müller, 1984)), we have $|sign\left\{\left(\hat{m}_{n,r-1}(X_i) - \hat{m}_{n,r-1}(X_k)\right)(X_i - X_k)\right\} - sign\left\{\left(m^{(r-1)}(X_i) - m^{(r-1)}(X_k)\right)(X_i - X_k)\right\}| = 0$, for all $n \geqslant n_0$, where n_0 is a fixed positive integer. The existence of n_0 is ensured by the definition of limit. Therefore,

$$
\begin{aligned}
&\sup_{t\in[0,1]} \sqrt{nh_n}|A_{n,r}(t) - B_{n,r}(t)| \\
&\leqslant \sup_{t\in[0,1]} \frac{\sqrt{nh_n}}{n(n-1)h_n^2} \sum_{1\leq k\neq i<n_0} \Big| sign\left\{\left(\hat{m}_{n,r-1}(X_i) - \hat{m}_{n,r-1}(X_k)\right)(X_i - X_k)\right\} \\
&- sign\left\{\left(m^{(r-1)}(X_i) - m^{(r-1)}(X_k)\right)(X_i - X_k)\right\} \Big| K\left(\frac{X_i - t}{h_n}\right) K\left(\frac{X_k - t}{h_n}\right) \\
&+ \sup_{t\in[0,1]} \frac{\sqrt{nh_n}}{n(n-1)h_n^2} \sum_{k\neq i\geqslant n_0} \Big| sign\left\{\left(\hat{m}_{n,r-1}(X_i) - \hat{m}_{n,r-1}(X_k)\right)(X_i - X_k)\right\} \\
&- sign\left\{\left(m^{(r-1)}(X_i) - m^{(r-1)}(X_k)\right)(X_i - X_k)\right\} \Big| K\left(\frac{X_i - t}{h_n}\right) K\left(\frac{X_k - t}{h_n}\right) \\
&\leqslant \sup_{t\in[0,1]} \frac{2\sqrt{nh_n}}{n(n-1)h_n^2} \sum_{1\leq k\neq i<n_0} K\left(\frac{X_i - t}{h_n}\right) K\left(\frac{X_k - t}{h_n}\right) \\
&\leqslant \frac{2\sqrt{nh_n}}{n(n-1)h_n^2} n_0(n_0-1)M_1^2 \to 0, \text{ as } n \to \infty,
\end{aligned}
$$

where $M_1 = \sup_x K(x)$, since n_0 is a fixed integer. This completes the proof. □

Proof of Theorem 3.1

Proof. Let $B_{n,r}(t)$ be the same as defined in the statement of Lemma 5.4 and $A_{n,r}(t)$ be the same as defined in Section 2. Then, by Lemma 5.6 we have $\sup_{t\in[0,1]} \sqrt{nh_n}|A_{n,r}(t)-B_{n,r}(t)| \xrightarrow{\mathrm{P}} 0$ as $n \to \infty$. Moreover, Lemma 5.5 asserts that,

$$\sup_{t\in[0,1]} \left| \sqrt{nh_n} \left(B_{n,r}(t) - E\left[B_{n,r}(t)\right]\right) - G_n(t) \right| \xrightarrow{\mathrm{P}} 0, \text{ as } n \to \infty,$$

where $G_n(t)$ is same as defined in Theorem 3.1. Using these two facts along with an application of continuous mapping theorem, we have

$$\sup_{t\in[0,1]} \left| M\left(\sqrt{nh_n} \left[A_{n,r}(t) - E[A_{n,r}(t)]\right] \right) - M(G_n(t)) \right| \xrightarrow{\mathrm{P}} 0$$

as $n \to \infty$ as $M(.)$ is a continuous functional. This completes the proof. □

Lemma 5.7. *Let $A_{n,r}(t)$ be as defined in* (3)*, and*

$$g_n(t) = \frac{1}{n^2} \sum_{1\leqslant i\neq j\leqslant n} \frac{1}{h_n} K\left(\frac{x_i - t}{h_n}\right) \frac{1}{h_n} K\left(\frac{x_j - t}{h_n}\right).$$

Then under the assumptions (A1) - (A4) and A(6), we have

$$\sup_{t\in[0,1]} \sqrt{nh_n} \left|g_n(t) - E_{H_0}(A_{n,r}(t))\right| \xrightarrow{P} 0 \text{ as } n \to \infty.$$

Proof. To prove this lemma, it is enough to show that $\sup_{t\in[0,1]} \sqrt{nh_n} \left|g_n(t) - E\left[B_{n,r}(t)\right]\right| \to 0$ in probability as $n \to \infty$, since

$$\sup_{t\in[0,1]} \sqrt{nh_n}|A_{n,r}(t) - B_{n,r}(t)| \xrightarrow{\mathrm{P}} 0, \tag{15}$$

as $n \to \infty$.

Note that

$$\begin{aligned}
&\sup_{t\in[0,1]} \sqrt{nh_n}|g_n(t) - E_{H_0}B_{n,r}(t)| \\
&= \sup_{t\in[0,1]} \frac{\sqrt{nh_n}}{n(n-1)} \left| \sum_{1\leqslant i\neq j\leqslant n} k_n(x_i - t)k_n(x_k - t) - \sum_{1\leqslant i\neq j\leqslant n} E_{H_0}[b_{n,t}(x_i, x_k)] \right| \\
&= \sup_{t\in[0,1]} \frac{\sqrt{nh_n}}{n(n-1)} \left| \sum_{1\leqslant i\neq j\leqslant n} k_n(x_i - t)k_n(x_k - t) \left(1 - E_{H_0} sign\left\{\left(m^{(r-1)}(x_i) - m^{(r-1)}(x_k)\right)(x_i - x_k)\right\}\right) \right| = 0.
\end{aligned} \tag{16}$$

Combining equations (15) and (16), we have

$$\sup_{t\in[0,1]} \sqrt{nh_n}\,|g_n(t) - E_{H_0}(A_{n,r}(t))| \xrightarrow{\mathrm{P}} 0 \text{ as } n \to \infty.$$

This completes the proof. □

References

Barlow, R. E., Bartholomew, D. J., Bremmer, J. M., & Brunk, H. D. (1972). *Statistical inference under order restrictions: The theory and application of isotonic regression.* Wiley, Chichester.

Barlow, R. E., & Brunk, H. D. (1972). The isotonic regression problem and its dual. *Journal of the American Statistical Association*, *67*(337), 140–147.

Best, M. J., & Chakravarti, N. (1990). Active set algorithms for isotonic regression; a unifying framework. *Mathematical Programming*, *47*(1-3), 425–439.

Bhattacharya, G. K., & Klotz, J. H. (1966). *The bivariate trend of lake mendota* (Tech. Rep.). No. 98, Department of Statistics, University of Wisconsin. (Available: https://cran.r-project.org/web/packages/isotone/isotone.pdf)

Billingsley, P. (2008). *Probability and measure*. John Wiley & Sons.

Brunk, H. D. (1955). Maximum likelihood estimates of monotone parameters. *The Annals of Mathematical Statistics*, 607–616.

Dette, H., Neumeyer, N., & Pilz, K. F. (2006). A simple nonparametric estimator of a strictly monotone regression function. *Bernoulli*, *12*(3), 469–490.

Dhar, S. S. (2016). Trimmed mean isotonic regression. *Scandinavian Journal of Statistics*, *43*(1), 202–212.

Dhar, S. S., Chakraborty, B., & Chaudhuri, P. (2014). Comparison of multivariate distributions using quantile–quantile plots and related tests. *Bernoulli*, *20*(3), 1484–1506.

Dykstra, R. L. (1981). An isotonic regression algorithm. *Journal of Statistical Planning and Inference*, *5*(4), 355–363.

Dykstra, R. L., & Robertson, T. (1982). An algorithm for isotonic regression for two or more independent variables. *The Annals of Statistics*, *10*(3), 708–716.

Easton, G. S., & McCulloch, R. E. (1990). A multivariate generalization of quantile-quantile plots. *Journal of the American Statistical Association*, *85*(410), 376–386.

Friedman, J. H., & Rafsky, L. C. (1981). Graphics for the multivariate two-sample problem. *Journal of the American Statistical Association*, *76*(374), 277–287.

Gasser, T., & Müller, H.-G. (1984). Estimating regression functions and their derivatives

by the kernel method. *Scandinavian Journal of Statistics*, 171–185.

Georgiev, A. A. (1984). Kernel estimates of functions and their derivatives with applications. *Statistics & Probability Letters*, *2*(1), 45–50.

Ghosal, S., Sen, A., & Van Der Vaart, A. W. (2000). Testing monotonicity of regression. *The Annals of Statistics*, 1054–1082.

Hildreth, C. (1954). Point estimates of ordinates of concave functions. *Journal of the American Statistical Association*, *49*(267), 598–619.

Lee, A. J. (1990). *U-statistics: Theory and practice*. Routledge.

Lee, C.-I. C. (1981). The quadratic loss of isotonic regression under normality. *The Annals of Statistics*, 686–688.

Lee, C.-I. C. (1983). The min-max algorithm and isotonic regression. *The Annals of Statistics*, 467–477.

Lim, E., & Glynn, P. W. (2012). Consistency of multidimensional convex regression. *Operations Research*, *60*(1), 196–208.

Marden, J. I. (1998). Bivariate qq-plots and spider web plots. *Statistica Sinica*, 813–826.

Marden, J. I. (2004). Positions and qq plots. *Statistical Science*, *19*(4), 606–614.

Ruppert, D., Wand, M. P., & Carroll, R. J. (2003). *Semiparametric regression*. Cambridge University Press.

Serfling, R. J. (2009). *Approximation theorems of mathematical statistics* (Vol. 162). John Wiley & Sons.

Varian, H. R. (1992). *Microeconomic analysis*. W.W. Norton & Company, New York.